frontiers | Frontiers in Earth Science

TYPE Original Research
PUBLISHED 02 September 2022
DOI 10.3389/feart.2022.921529

OPEN ACCESS

EDITED BY
Daniel R. Parsons,
University of Hull, United Kingdom

REVIEWED BY
Quanzhong Guan,
Chengdu University of Technology, China
Zhiye Gao,
China University of Petroleum, China

*CORRESPONDENCE
Yao Du,
404298823@qq.com

SPECIALTY SECTION
This article was submitted to Sedimentology, Stratigraphy and Diagenesis, a section of the journal Frontiers in Earth Science

RECEIVED 16 April 2022
ACCEPTED 09 August 2022
PUBLISHED 02 September 2022

CITATION
Du Y, Wang X, Zhao R, Chen C, Wen S, Tang R, Mo Q, Zhang J, Zhang Y and He S (2022), Controlling factors of organic matter enrichment in continental shale: A case study of the Jurassic Da'anzhai member in the Sichuan Basin.
Front. Earth Sci. 10:921529.
doi: 10.3389/feart.2022.921529

Controlling factors of organic matter enrichment in continental shale: A case study of the Jurassic Da'anzhai member in the Sichuan Basin

Yao Du[1,2,3]*, Xingzhi Wang[1,3], Rongrong Zhao[2], Chi Chen[2], Siying Wen[2], Ruifeng Tang[2], Qianwen Mo[2], Jizhi Zhang[2], Yu Zhang[2] and Shuo He[4]

[1]State Key Laboratory of Oil and Gas Reservoir Geology and Exploitation, Southwest Petroleum University, Chengdu, China, [2]Exploration Division of PetroChina Southwest Oil and Gasfield Company, Chengdu, China, [3]School of Geoscience and Technology, Southwest Petroleum University, Chengdu, China, [4]Research Institute of Geologic Exploration and Development, Chuanqing Drilling and Exploration Corporation, CNPC, Chengdu, China

The continental lake basin is a favorable accumulation area of shale oil and gas; however, the organic matter enrichment regularity in continental lake facies is still controversial, which hinders the exploration of continental shale oil and gas in the Sichuan Basin. In this study, the relationship between a sedimentary environment and organic matter enrichment of continental shale was analyzed by petrology and organic and inorganic geochemistry tests of 153 samples. The results show that different lithologic associations in the Da'anzhai member have different contents of organic matter. Among them, the TOC content of unit II (shale-limestone interbed) is the highest, mainly, type II kerogen, followed by unit III (shale clip shell limestone belts), mainly, type III kerogen. Geochemical indicators show that different paleoenvironmental factors play different leading roles in organic matter enrichment in different periods of the Da'anzhai member. Unit II is deposited in an arid environment with less fresh water supply; therefore, the water cycle is hampered. Due to the effect of salinity stratification, anoxic water was formed, which was beneficial to the preservation of algae and plankton in the lake basin, resulting in the formation of type II_2 kerogen. Unit III is deposited in a semi-humid and semi-arid climate, and its water is in an oxidizing environment. Precipitation and river runoff increase the input of terrigenous debris and higher plants to form type III kerogen. This study has guiding significance for the cause of organic matter enrichment in the Da'anzhai member and the prediction of favorable zones.

KEYWORDS

lacustrine shale, paleoenvironment, organic matter enrichment model, sichuan basin, Da'anzhai member

1 Introduction

Organic shales include mud shale formations, thin layers of tight sandstone, carbonate rocks, and even volcanic rocks (Zhang et al., 2012). Organic shales not only record the evolution of ancient life, paleoclimate, evolution characteristics of paleoenvironment such as lakes and oceans (Loucks and Ruppel, 2007) but are also the carrier of mineral resources such as oil and gas, which has important economic benefits. Marine shale has become the focus of exploration, and lacustrine shale has great exploration potential. However, no progress has been made in the oil and gas exploration of continental shale in the Sichuan Basin due to people's different opinions on the enrichment patterns of organic matter (Jiao, 2019; Zou et al., 2019; Hu et al., 2021).

The main arguments of domestic and foreign scholars on the main factors of organic matter enrichment can be summarized as "organic matter production," "decomposition and preservation," and "dilution" (Demaison and Moore, 1980; Pedersen and Calvert, 1990; Zhang et al., 2016). Around these three models, many scholars have studied lithology difference (Mayer et al., 1985), deposition rate (Calvert, 1987), terrigenous debris injection, tectonic activity, and climate change (Bluth and Kump, 1994; Huang et al., 2020; Xu et al., 2021), and even some special geological events, such as marine transgression and anoxia to study the factors of shale organic matter enrichment. The paleosedimentary environment controls the primary productivity and preservation conditions of the basin to a certain extent, and sedimentary geochemistry records the characteristics and evolution information of the paleoenvironment. Therefore, major and trace elements are often used for paleoenvironmental reconstruction (Tribovillard et al., 2006, 2012). From the previous studies on continental shale, many research results focused on lacustrine environments such as drought, salinization, and wetting, and achieved many exploration results (Wei et al., 2012; Huang et al., 2020; Wang et al., 2021). However, the study of continental shale in the Sichuan Basin is very weak.

In December 2020, China National Petroleum Company (CNPC) deployed Well C, a shale oil exploration well in the Sichuan Basin, and carried out coring in the Da'anzhai member; for this set of cores, we conducted intensive sampling, which provides the possibility for the detailed study of the covariation of sedimentary environment evolution and organic matter enrichment patterns. In addition, we analyzed paleoclimate, paleo-weathering, detrital inflow, paleo-salinity, and paleo-redox conditions based on organic and inorganic geochemistry, to clarify the relationship between a lake sedimentary environment, evolution, and organic matter enrichment regularity in the Da'anzhai member.

2 Regional geological background

The Sichuan Basin is a foreland and craton superimposed basin on the northwest side of the Yangzi quasi platform. It has become a plate or craton basin in western South China since the new Proterozoic era (Sinian) and lasted until the late Middle Triassic. Through the Indosinian orogenic movement, the Sichuan Basin has developed into a new foreland basin since the late Triassic, forming six structural areas bounded by the Longquan Mountain deep fracture and Huaying Mountain deep fracture (Li and He, 2014; Li et al., 2020) (Figure 1A). Sedimentary facies studies show that there are three ancient continents around the Sichuan Basin in the late Triassic, namely, Longmenshan, Daba Mountain, and Kangdian (Liu, 1993). Under this paleotectonic-sedimentary background, the Jurassic continued to deposit based on the late Triassic lake basin and developed into a delta-inland lake. The inland lake includes sedimentary micro-facies such as lake slope mud, semi-deep lake mud, gravity flow, and debris beach (Figure 1B); its sedimentation center is distributed from central Sichuan to eastern Sichuan, containing bivalves and plant and alga fossils (Meng et al., 2005; Tong et al., 2016; Deng et al., 2017).

The Da'anzhai member is in the Toarcian Stage, Ziliujing group, in the late early Jurassic. The sedimentary period of the Da'anzhai member is in the marine regression after the global marine transgression. The long-term lake regression in the sedimentary period of the Da'anzhai member is consistent with the change in the global sea level in time, which corresponds to a complete regional lake transgression–regression depositional cycle (Zheng, 1998; Liu et al., 2020). According to the fluctuation of the lake level, the lake level of units IV–III rises, the top of unit III is on the maximum flooding surface, and the whole units II–I are in the process of lake regression (Figure 1B).

3 Experimental methods

3.1 Sample analysis

This analysis includes 153 samples from Well A, Well B, Well C, and Well D. The analytical item of the 111 samples from wells A, B, and D is rock slice and the analytical item of Well C is rock-eval pyrolysis and major and trace elements. A total of 42 samples from Well B were ground into 80 mesh and less than 200 mesh powder separately for chemical analysis. The 80 mesh samples were used for the analysis of total organic carbon (TOC) and rock-eval pyrolysis (S_1, S_2, and Tmax). The TOC was measured by the LECO CS230 carbon and sulfur analyzer, and the S_1, S_2, and Tmax data were measured by the oil and gas show and evaluation unit, YQ-VIIA. This work was completed in the analysis and experimental center of the Institute of Exploration and Development, Southwest Oil and Gas Field Company. Samples of less than 200 mesh were used for the analysis of major and trace elements. An EDX5500H energy scattering X-ray fluorescence spectrometer was used to detect the major and trace elements, which was completed in Chuanqing

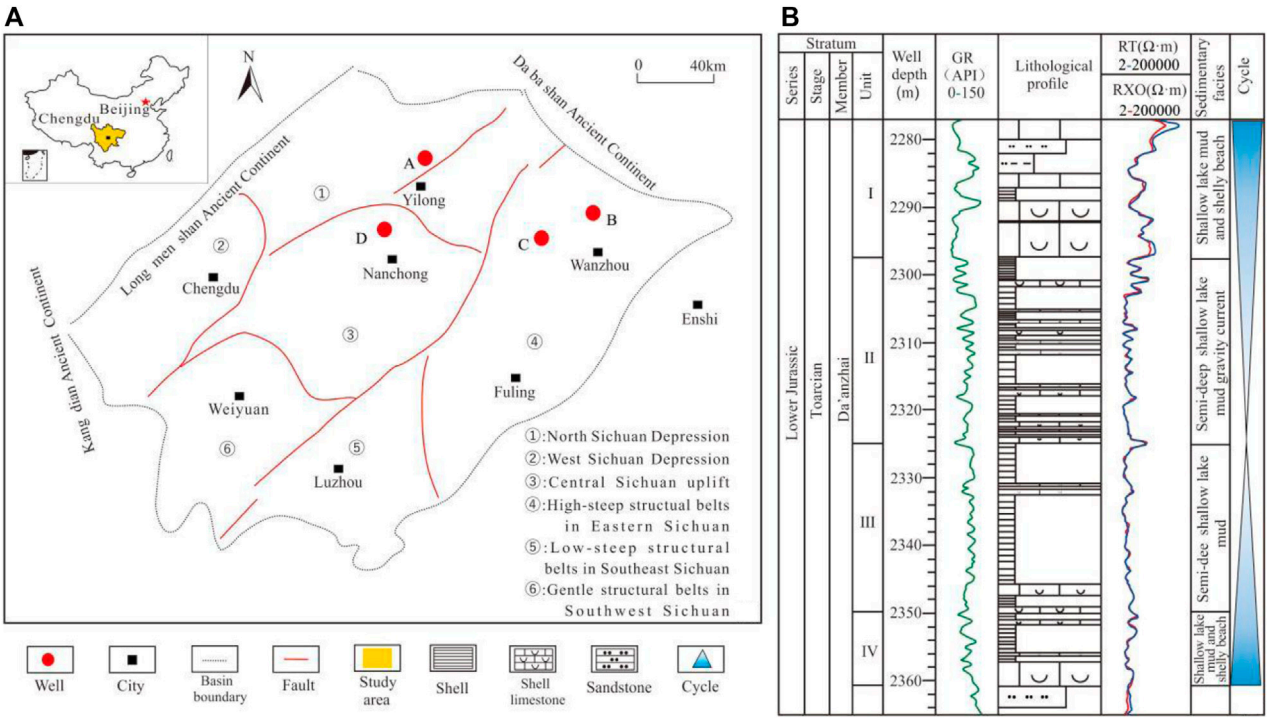

FIGURE 1
Structural location of the research area **(A)** and formation histogram of well C **(B)**.

Drilling Geological Exploration and Development Research Institute (Table 1). Mineral content was obtained by lithology scanning (LITHOSCANNER) logging of Schlumberger Company, and the inline resolution of this equipment was 18 feet, and the detection depth was 9 feet.

3.2 Data processing

Using the content of post-Archean Australian shale (PAAS) as the reference standard, if the content of an element in the sediment is significantly higher than the average shale content, it indicates that this element is of authigenic enrichment; otherwise, it is relative depletion (Taylor and Mclennan, 1985). Some biogenic carbonate minerals can dilute authigenic minerals in sediments, which can be reduced by Al standardization (Wedepohl, 1971; Tribovillard et al., 2006). The enrichment factor (EF) can quantitatively analyze the enrichment degree of an element (Turekian and Wedepohl, 1961; Wedepohl, 1971).

$$X_{EF} = (X/Al)_{sample} / (X/Al)_{average\ shale} \quad (1)$$

.

The trace element X is of more enrichment when X_{EF} element >1; the trace element X is relative depletion when X_{EF} element <1 (Wedepohl, 1971; Tribovillard et al., 2006).

Ba biology (Ba_{bio}) is related to phytoplankton decay, which has been proved to be a reliable indicator of paleoproductivity (Dymond et al., 1992).

$$Ba_{bio} = Ba_{sample} - (Al_{sample} \times Ba/Al_{alu}) \quad (2)$$

Ba_{sample} and Al_{sample} are the quality fraction of the measured samples. Ba/Al_{alu} represents the terrestrial input part of sediments, and 0.0075 is generally used to calculate the Ba biological content (Dymond et al., 1992).

4 Results

4.1 Sedimentary characteristics

Sedimentology research plays a strong indicative role in clarifying the water environment of the lake basin. The author analyzes the petrological characteristics and paleontology of the Da'anzhai member to clarify the water environment of the Da'anzhai member.

4.1.1 Unit IV

Lithologic associations are interbedded with micritic shell limestone and thin shale (Figure 2A). Lithology scanning showed

TABLE 1 Measured values of TOC and major elements in Da'anzhai shale of well C [PAAS data from Taylor and Mclennan (1985)].

Stratum	Depth (m)	TOC	Fe_2O_3	Al_2O_3	SiO_2	K_2O	CaO	TiO_2	MgO	P_2O_5	MnO	Na_2O	Ba	V	Sr	Cr	Th	U	Cu	Co	Ni	Mo
		%	%	%	%	%	%	%	%	%	%	%	ppm	ppm	ppm	ppm	ppm	ppm	ppm	ppm	ppm	ppm
PAAS			3.05	9.97	27.91	1.92	23.87	0.63	0.69	0.72	0.07	0.11	648.01	158.10	377.45	64.30	6.03	1.60	23.51	6.49	62.45	0.35
I	2278		3.09	11.55	39.95	1.88	22.52	0.57	0.54	0.38	0.12	0.10	526.85	109.80	202.83	81.56	7.05	1.63	19.53	6.89	7.29	0.41
	2280	0.32	3.79	14.15	45.79	2.08	18.19	0.58	0.99	0.32	0.07	0.16	768.11	200.98	206.53	126.24	9.75	1.96	28.44	8.99	32.56	0.42
	2282	0.49	4.95	15.90	54.14	2.58	9.63	0.99	1.35	0.26	0.07	0.27	330.86	184.15	503.83	81.18	8.58	1.89	39.66	14.61	40.73	0.50
	2284	0.28	4.82	14.72	43.96	2.54	15.67	0.89	1.12	0.36	0.05	0.23	436.69	104.52	292.61	25.73	0.81	0.88	32.30	13.27	13.94	0.42
	2286		1.82	5.36	15.98	1.39	40.71	0.33	0.12	0.53	0.06	0.09	471.31	106.16	416.50	42.11	7.53	1.75	10.45	0.00	0.00	0.27
	2288		2.84	9.09	28.28	2.04	28.05	0.49	0.23	0.48	0.05	0.10	603.46	107.06	260.96	71.39	8.16	1.96	21.71	4.70	15.51	0.40
	2290	0.53	4.82	14.76	42.78	2.59	15.89	0.62	1.14	0.33	0.06	0.16	464.61	67.67	275.79	47.73	4.94	1.54	28.02	10.96	38.78	0.42
	2292	0.57	3.02	10.90	31.52	2.06	27.23	0.40	0.58	0.43	0.04	0.10	401.92	48.65	345.30	31.80	4.49	1.35	20.43	5.52	11.07	0.37
	2294		2.70	8.41	24.70	1.91	32.47	0.28	0.19	0.48	0.03	0.09	372.71	41.68	472.14	16.09	2.09	1.06	18.25	2.78	9.02	0.32
	2296		1.66	5.36	15.70	1.26	40.07	0.17	0.37	0.53	0.01	0.09	383.59	90.43	474.06	39.99	4.08	1.35	10.83	0.00	0.00	0.27
II	2298	1.47	2.71	7.61	21.00	1.96	36.09	0.38	0.28	0.50	0.02	0.09	1004.50	245.15	437.45	73.82	3.93	1.42	20.32	3.25	7.18	0.32
	2300	1.82	2.79	10.10	28.81	2.19	26.32	0.83	0.76	0.47	0.04	0.10	593.35	109.60	469.41	39.38	4.50	1.41	21.05	3.95	13.02	0.34
	2302	2.50	2.67	9.52	27.53	2.15	28.12	0.43	0.63	0.48	0.03	0.10	672.93	97.80	515.34	40.14	4.77	1.37	19.32	2.91	3.34	0.33
	2304	1.75	2.70	9.18	25.82	2.07	29.85	0.42	0.85	0.48	0.03	0.10	587.26	85.55	519.84	40.82	4.40	1.51	16.56	3.28	7.39	0.34
	2306	1.39	2.79	9.61	28.12	2.06	28.58	0.38	0.90	0.48	0.04	0.10	527.76	73.25	512.76	38.47	4.26	1.39	17.29	4.01	2.85	0.34
	2308	0.79	2.78	8.94	26.08	1.95	31.01	0.35	0.65	0.49	0.04	0.09	669.28	125.88	531.39	62.97	4.59	1.48	16.70	3.86	12.59	0.34
	2310	1.05	2.96	10.53	29.14	2.10	27.68	0.51	0.77	0.47	0.04	0.10	645.99	120.70	541.34	51.44	5.43	1.60	20.53	5.24	16.97	0.34
	2312	0.89	2.96	10.71	29.67	2.10	27.40	0.51	0.78	0.46	0.04	0.10	652.84	133.65	479.56	48.56	3.24	1.27	22.85	5.32	16.38	0.35
	2314	1.50	2.70	8.65	24.89	1.91	32.60	0.47	0.50	0.48	0.04	0.10	692.10	125.73	541.35	46.21	3.90	1.56	17.29	3.00	2.31	0.29
	2316	1.24	2.82	8.59	25.54	1.94	30.60	0.46	0.63	0.55	0.04	0.09	522.89	78.63	571.10	32.78	3.31	1.26	19.29	4.08	5.88	0.31
	2318	1.61	2.67	7.74	22.40	1.76	34.51	0.32	0.23	0.57	0.03	0.09	583.30	84.50	595.70	32.71	3.38	1.38	16.49	2.61	10.10	0.29
	2320	1.47	2.72	7.94	22.03	1.85	33.79	0.33	0.21	0.56	0.02	0.09	637.85	103.32	552.32	34.53	3.33	1.32	17.42	3.09	0.00	0.30
	2322	1.54	2.67	6.67	19.61	1.52	36.25	0.38	0.00	0.64	0.02	0.09	900.64	185.29	581.71	54.78	2.74	1.21	18.12	3.03	10.48	0.29
	2324	/	2.74	6.82	19.99	1.51	35.69	0.58	0.00	0.64	0.03	0.09	1134.52	289.17	501.35	75.79	4.75	1.43	18.50	3.75	11.29	0.27
	2326	/	3.05	8.10	23.64	1.81	30.51	0.98	0.20	0.57	0.04	0.09	639.22	129.22	303.83	67.75	7.77	1.76	20.70	6.23	13.02	0.31
III	2328	0.84	4.21	14.36	37.18	2.50	19.86	0.61	1.12	0.39	0.04	0.12	568.01	92.42	260.07	59.41	7.04	1.64	28.54	10.17	25.95	0.41
	2330	0.86	3.94	14.70	37.26	2.46	21.36	0.51	1.14	0.37	0.03	0.14	728.16	146.20	391.77	63.88	6.22	1.54	25.99	9.19	27.96	0.39
	2332	0.98	3.40	13.15	33.74	2.26	23.54	0.61	0.96	0.43	0.03	0.11	630.17	108.90	372.25	64.79	6.54	1.67	22.50	7.45	17.30	0.37
	2334	0.32	4.02	14.30	36.31	2.38	21.43	0.54	1.06	0.41	0.03	0.13	641.28	109.35	319.03	66.01	7.51	1.73	33.65	9.33	25.52	0.40
	2336	0.59	4.52	15.00	38.61	2.61	18.72	0.57	1.22	0.39	0.03	0.15	581.78	105.12	324.52	64.95	8.36	1.88	31.86	11.07	32.18	0.39
	2338	0.47	4.64	15.55	41.00	2.80	16.51	0.57	1.32	0.37	0.03	0.16	606.81	100.14	291.06	75.26	7.82	1.94	32.68	11.45	33.15	0.41

(Continued on following page)

10.3389/feart.2022.921529

10.3389/feart.2022.921529

TABLE 1 (*Continued*) Measured values of TOC and major elements in Da'anzhai shale of well C [PAAS data from Taylor and Mclennan (1985)].

Stratum	Depth (m)	TOC	Fe_2O_3	Al_2O_3	SiO_2	K_2O	CaO	TiO_2	MgO	P_2O_5	MnO	Na_2O	Ba	V	Sr	Cr	Th	U	Cu	Co	Ni	Mo
		%	%	%	%	%	%	%	%	%	%	%	ppm	ppm	ppm	ppm	ppm	ppm	ppm	ppm	ppm	ppm
	2340	0.36	4.84	15.92	41.84	2.92	15.99	0.59	1.34	0.35	0.04	0.18	557.21	154.47	384.59	71.24	5.98	1.53	34.27	12.12	35.15	0.42
	2342	0.49	4.22	13.30	34.30	2.23	24.27	0.97	0.97	0.49	0.05	0.16	532.33	146.25	384.03	59.10	6.20	1.51	27.75	9.39	28.17	0.35
	2344	/	4.15	12.99	33.81	2.21	24.64	0.98	0.93	0.48	0.05	0.14	497.25	67.37	214.59	56.37	7.96	1.89	23.81	9.35	23.09	0.37
	2346	/	3.97	15.40	40.70	2.59	18.77	0.46	1.35	0.36	0.03	0.15	515.28	68.32	302.17	39.91	5.70	1.54	30.47	9.16	214.59	0.43
	2348	0.15	3.01	12.54	32.49	2.15	25.78	0.39	0.95	0.46	0.03	0.10	541.31	80.72	394.75	37.11	4.54	1.48	22.53	6.09	302.17	0.37
IV	2350	0.25	2.80	9.50	26.09	1.93	31.71	0.36	0.41	0.53	0.03	0.10	377.50	91.67	404.44	50.15	6.19	1.58	22.40	4.12	394.75	0.34
	2352	0.23	3.54	13.51	35.34	2.29	21.94	0.46	1.01	0.44	0.04	0.11	3556.16	1804.21	641.61	334.23	1.62	0.84	28.75	8.58	404.44	0.38
	2354	/	3.61	10.56	32.40	2.19	14.89	5.26	0.94	0.48	0.12	0.16	611.68	131.71	231.92	80.34	7.46	1.86	27.16	8.61	641.61	0.15
	2356	0.43	4.44	15.30	40.18	2.66	19.18	0.66	1.31	0.36	0.04	0.16	719.41	166.17	253.67	62.44	4.45	1.28	34.31	10.29	40.89	0.41
	2358	/	2.83	11.44	29.63	2.02	29.46	0.61	0.92	0.45	0.04	0.10	719.41	166.17	253.67	62.44	4.45	1.28	25.33	4.33	11.94	0.34

that the calcite content was the highest, with an average of 34.16%, followed by illite and chlorite, accounting for 18.99 and 9.02%, respectively (Figure 3), containing quartz particles (Figure 2B, Figure 3). The organisms are mainly single bivalves (Figure 2A), indicating shallow water deposition in this period.

4.1.2 Unit III

Lithological associations are pure black mud shale clip shell limestone belts (Figure 2C). Lithology scanning shows that the illite content is the highest, reaching 29.35%, followed by quartz content, accounting for 26.30%, and also contains pyrite (Figure 3). Most of the bio-particles are single ostracods (Figure 2D) and rare bivalve and gastropod debris fossils, showing that the lithologic association is a typical product of deep-water deposition and higher plants can be seen at times (Figure 2E).

4.1.3 Unit II

Lithologic associations are the interbedded strata of shale and shell limestone. Lithology scanning showed that the quartz content reached 35.72% and chlorite and illite content were similar, accounting for 23.85 and 22.05%, respectively (Figure 3). Bio-particles are mainly deformed bivalves (Figure 2F), usually of plastic deformation. The trace of algae (Figure 2G) (Figure 2H), indicates frequent biological activities in local layers, and sufficient food supply and high oxygen content in the sedimentary environment (Zhang et al., 2018).

4.1.4 Unitl

Lithologic associations are interbedded with micritic shell limestone and thin shale (Figure 2I). Lithology scanning shows that the calcite content reaches 44.97% and quartz content reaches 28.01% (Figure 3). The bivalve fragments of this layer are in the majority (2i), indicating that the shallow water sedimentary environment is the result of the long-term decline of the lake level in the late deposition of the Da'anzhai member.

4.2 Total organic carbon and organic matter type

TOC varies obviously in the vertical direction of the Da'anzhai member, with a distribution range of 0.15–2.5% and an average of 0.90%. The TOC in unit II is the highest, ranging from 0.79–2.5%, with an average of 1.46%, while that in unit IV is the lowest, ranging from 0.23–0.43%, with an average of 0.30%. The TOC in units I and III is moderate (Figure 4). It is worth noting that the TOC lower limit value of the effective source rock of lacustrine shale has not yet been unified at present, and CNPC has limited the effective source rocks for shale oil exploration in the Sichuan Basin to 1% (Zou et al., 2019; Zhao et al., 2020). Rock pyrolysis analysis showed that S_1 content is between 0.03 and 2.42 mg/g, with an average value of 0.65 mg/g,

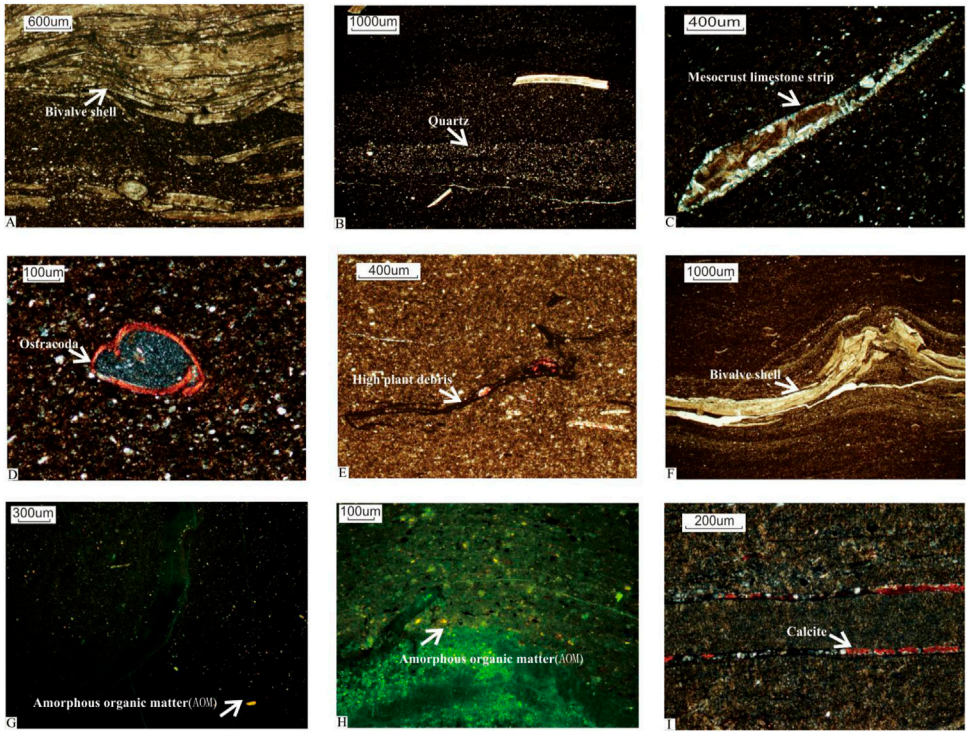

FIGURE 2
Micrographs of the Da'anzhai member **(A)** interbedded shale and limestone, bivalve shell, 3675.34 m, well A; **(B)** silt-bearing shale, 3672 m, well A; **(C)** pure black mud shale clip shell limestone belts, 3637.55 m; **(D)** silt-bearing calcareous mudstone, shale, ostracod, 3639.18 m, well A; **(E)** grapholith, higher plants, 3667.97 m, well A; **(F)** shale, bivalve shell, 1745.9 m, well B; **(G)** shale, amorphous organic matter (algae), 2432 m, well D; **(H)** shale, amorphous organic matter (algae), 2466 m, well D; **(I)** interbedded shale and limestone, 1720.99 m, well B

and S_2 content is between 0.12 and 3.12 mg/g, with an average value of 0.95 mg/g. By analyzing the relationship between Tmax and the hydrogen index, it can be found that the organic matter types in the Da'anzhai member are mainly type II_2 and type III with one sample distributed in zone II_1 (Figure 5A). In terms of the relationship between S_1 and TOC, in units IV–III and unit I, S_1 increases slowly with the increase in the TOC, indicating that type III kerogen is the main source of unit IV, unit III, and unit I, reflecting the source of higher terrestrial plants, while type II_2 kerogen is the main source of unit II (Figure 5B), reflecting the source of lower plankton.

4.3 Major elements

As shown in Table 1, the main enrichment components in the Da'anzhai member, the study area, are Fe_2O_3, Al_2O_3, SiO_2, K_2O, CaO, TiO_2, MgO, P_2O_5, and other major elements. Among them, SiO_2 is the most important component, ranging from 15.70–58.86%, with an average of 34.16%, followed by CaO, ranging from 3.79–40.71%, with an average of 23.80%, and Al_2O_3 is the lowest, ranging from 5.36–17.22%, with an average of 11.82%, while K_2O, TiO_2, MgO, P_2O_5, and MnO are all lower, with an average of less than 1%. Obviously, there are differences in the contents (average values) of major elements in different strata. There are more illite and chlorite in unit IV, and the content of Al is higher. There are more pyrite and quartz in the unit III, and the content of Fe and Si is higher. Frequent alternation of shale and limestone in unit II leads to higher Ca content, while more quartz and calcite particles and higher Si and Ca content in unit I (Table 1; Figure 3). Compared with PAAS (Turekian and Wedepohl, 1961), CaO, Fe_2O_3, TiO_2, and P_2O_5 are enriched in units I-IV of the Da'anzhai member, while SiO_2, K_2O, MgO, K_2O, and MnO are relatively depleted (Figure 6).

4.4 Trace elements

According to the results of this experiment, trace elements such as Ba, V, Cr, Th, U, Sr, Cu, Co, Ni, and Mo are mainly used to characterize the evolution of the paleoenvironment. Trace element contents (average values) in the Da'anzhai member showed significant variation, with Ba ranging from 1.63–3556.16 ppm (623 ppm), V from 1.74–1804.21

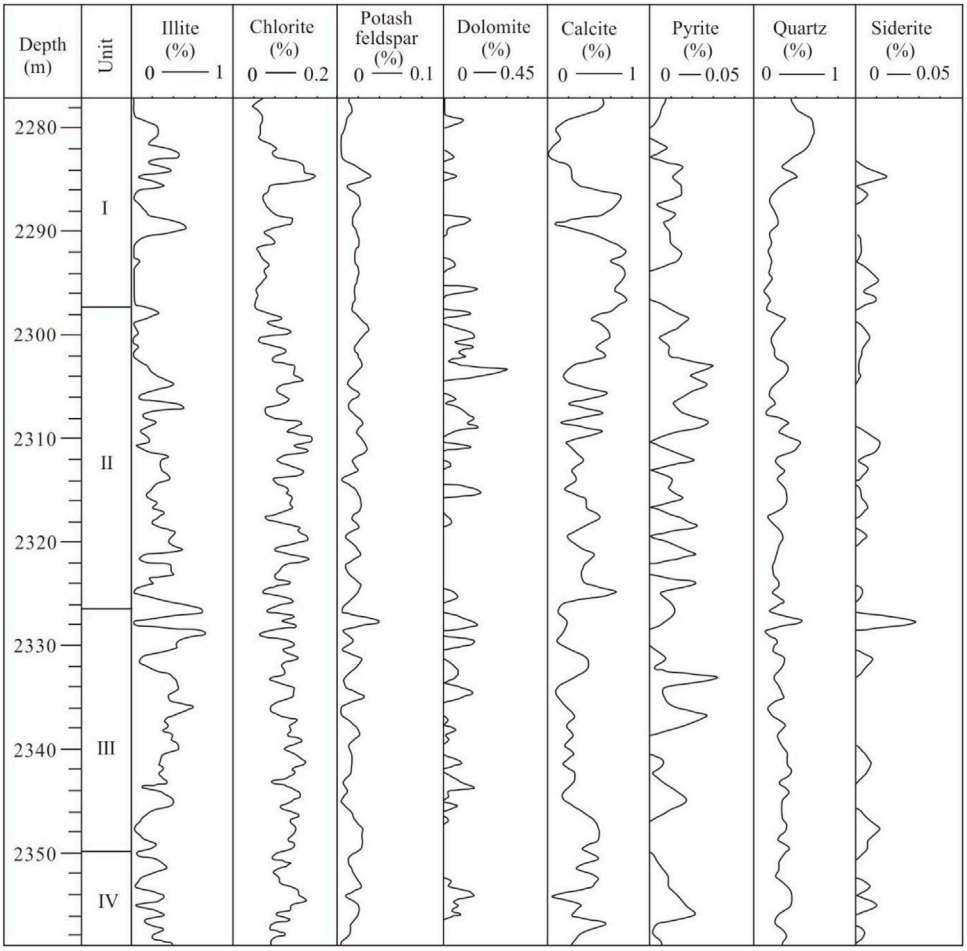

FIGURE 3
Mineral content in the Da'anzhai member of well C.

(687.21 ppm), Cr from 0.98–334.23 (59.00 ppm), Th from 0.64–12.00 ppm (5.26 ppm), U from 0.24–3.70 ppm (1.50 ppm), Sr from 1.91–641.61 ppm, Cu from 0.74–45.00 ppm, Co from 0.48–19.00 ppm (6.42 ppm), Ni from 1.30–641.61 (58.91ppm), and Mo from 0.06–2.6 ppm (0.39 ppm). Compared with PAAS (Turekian and Wedepohl, 1961), the 10 trace elements cited here are depleted in unit I; Ba, V, and Sr are faintly enriched in unit II, while in unit IV only V and Ni are enriched, and other elements are depleted (Figure 6).

5 Discussion

5.1 Paleoclimate

Climate, the main cause of the changes in the depositional environment, mainly affects parent rock weathering, sediment erosion and transport, and terrigenous detrital supply. Sr/Cu can be used to evaluate paleoclimate conditions. For arid and hot climates, the Sr/Cu ratio is above 5, while for warm and humid climates, the Sr/Cu ratio is between 1 and 5 (Turekian and Wedepohl, 1961; Moradi et al., 2016). This experiment shows that the ratio of Sr/Cu in the Da'anzhai member is greater than 5, which reflects that the whole Da'anzhai member is arid and hot. However, Sr may be quite abundant in continental lake basins (Wu et al., 2021), and the paleoclimate index calculated by Sr/Cu is larger than the actual one. Therefore, the conclusion of Sr/Cu may be more arid than the actual one.

Considering that Fe, Mn, Cr, Ni, V, and Co are generally enriched under humid conditions, while Ca, Mg, Sr, Ba, K, and Na are accumulated in an arid environment, Moradi et al. (2016) used C =Σ (Fe + Mn + Cr + Ni + V + Co)/Σ (Ca + Mg + Sr + Ba + K + Na) to characterize paleoclimate. C values of 0.6–0.8, 0.4–0.6, and 0.2–0.4 represent semi-humid, semi-arid and semi-humid, and semi-arid climates, respectively, while C values above 0.8 or below 0.2 reflect humid and arid paleoclimate environments, respectively. According to the change in the C value, the climate

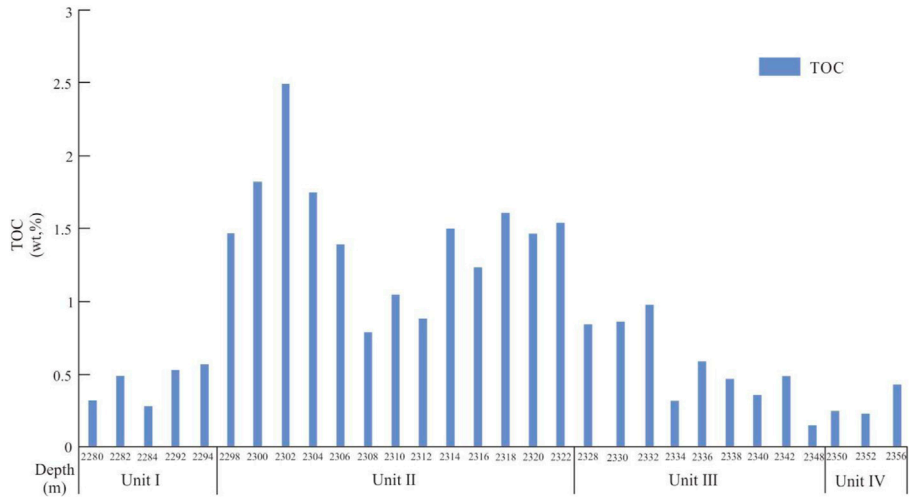

FIGURE 4
TOC distribution map in the Da'anzhai member of well C.

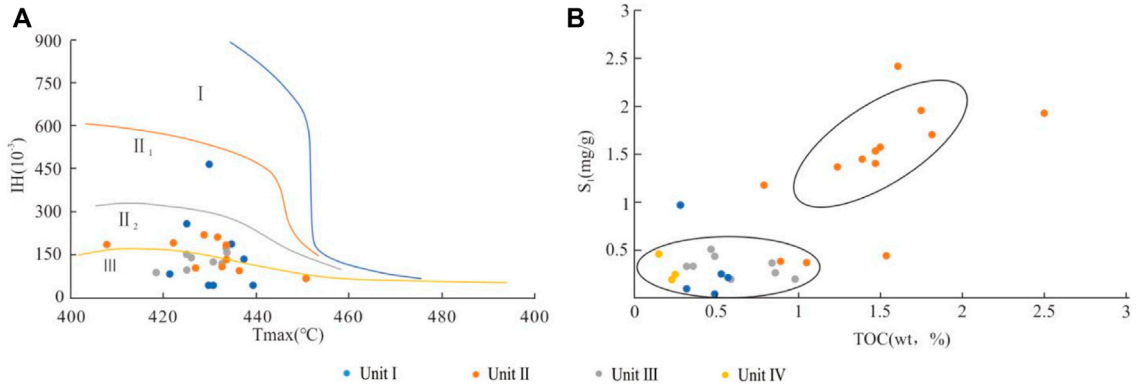

FIGURE 5
(A) Tmax-HI indicates the organic types in the Da'anzhai member; **(B)** S_1 is positively correlated with TOC.

of units IV–III in the study area is in the process of semi-humid to semi-arid, the climate of unit II becomes arid, and the climate of unit I gradually becomes humid from arid (Figure 7). Previous studies have shown that the relatively humid environment is beneficial to the development of higher plants (Jinhua et al., 2018), which is consistent with the observation of the higher plants in unit III in this study (Figure 2E).

On the whole, the TOC has a negative correlation with the C value, indicating that organic matter is enriched under drought conditions (Figure 8A). From the relationship between the TOC and C values of each unit (Figure 8B), the correlation between TOC and C values is quite different in different sedimentary periods. The enrichment degree of organic matter in unit II is higher than that in other periods, but there is no correlation between TOC and C values in unit II. It is inferred that the drought condition is not the only factor leading to organic matter enrichment in this period.

5.2 Paleoweathering

The chemical index of alteration (CIA) is an index indicating the degree of chemical weathering, which is affected by climate. A warm and humid climate will lead to stronger weathering and higher CIA value (Nesbitt and Young, 1982). CIA = {x (Al_2O_3)/[x (Al_2O_3) + x (CaO*) + x (Na_2O) + x (K_2O)]} × 100. The unit for each of the aforementioned main components is the number of

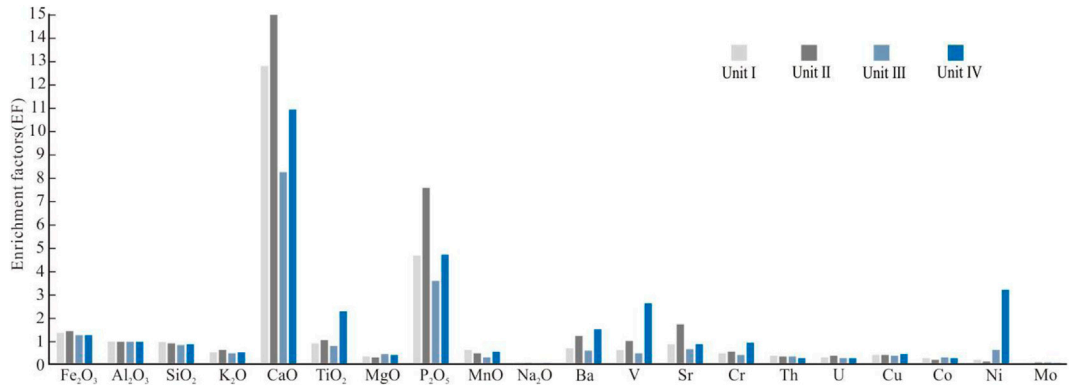

FIGURE 6
Enrichment coefficient of major elements in the Da'anzhai member of well C.

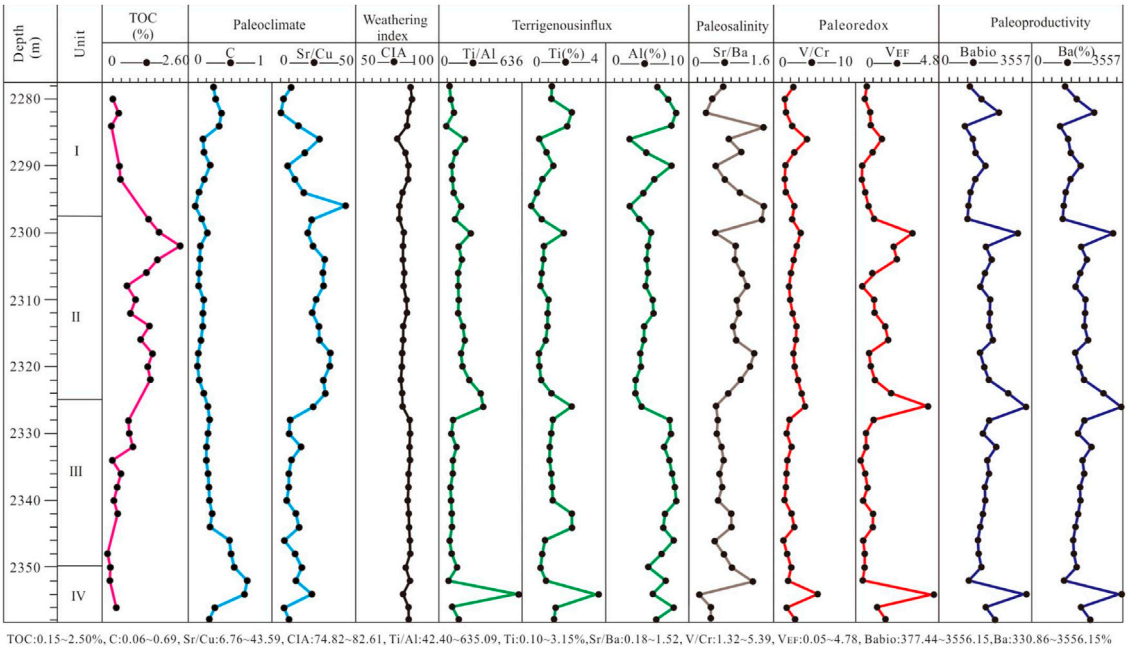

FIGURE 7
Paleoenvironment parameter in the Da'anzhai member of well C.

moles. CaO* is calculated by the calibration method proposed by McLennan et al. (1993). It is assumed that the Ca/Na ratio of silicate minerals in nature is 1. First, the CaO content of the sample is subtracted from the P_2O_5 content to ensure the removal of Ca in phosphate. Then, the CIA is calculated according to the molar ratio of CaO/Na_2O in the sample. A ratio greater than 1 implies the presence of chemically deposited carbonates, in which case the molar content of Na_2O is used instead of the CaO content. A ratio less than 1 indicates that there is no carbonate mineral, in which case the CaO molar content is directly used as the CaO content. A CIA in the range of 50–60 represents low weathering, a CIA in the range of 60–80 represents moderate weathering, and a CIA above 80 represents strong weathering.

The CIA of unit IV-III is generally 78.38 to 82.61 (Figure 7), with an average of 81.64. The weathering degree was strong in this period, which is consistent with the humid climate in this period. However, the CIA of unit II is generally lower than 80, with an average of 78.31, indicating that the weathering degree is relatively weak in an arid

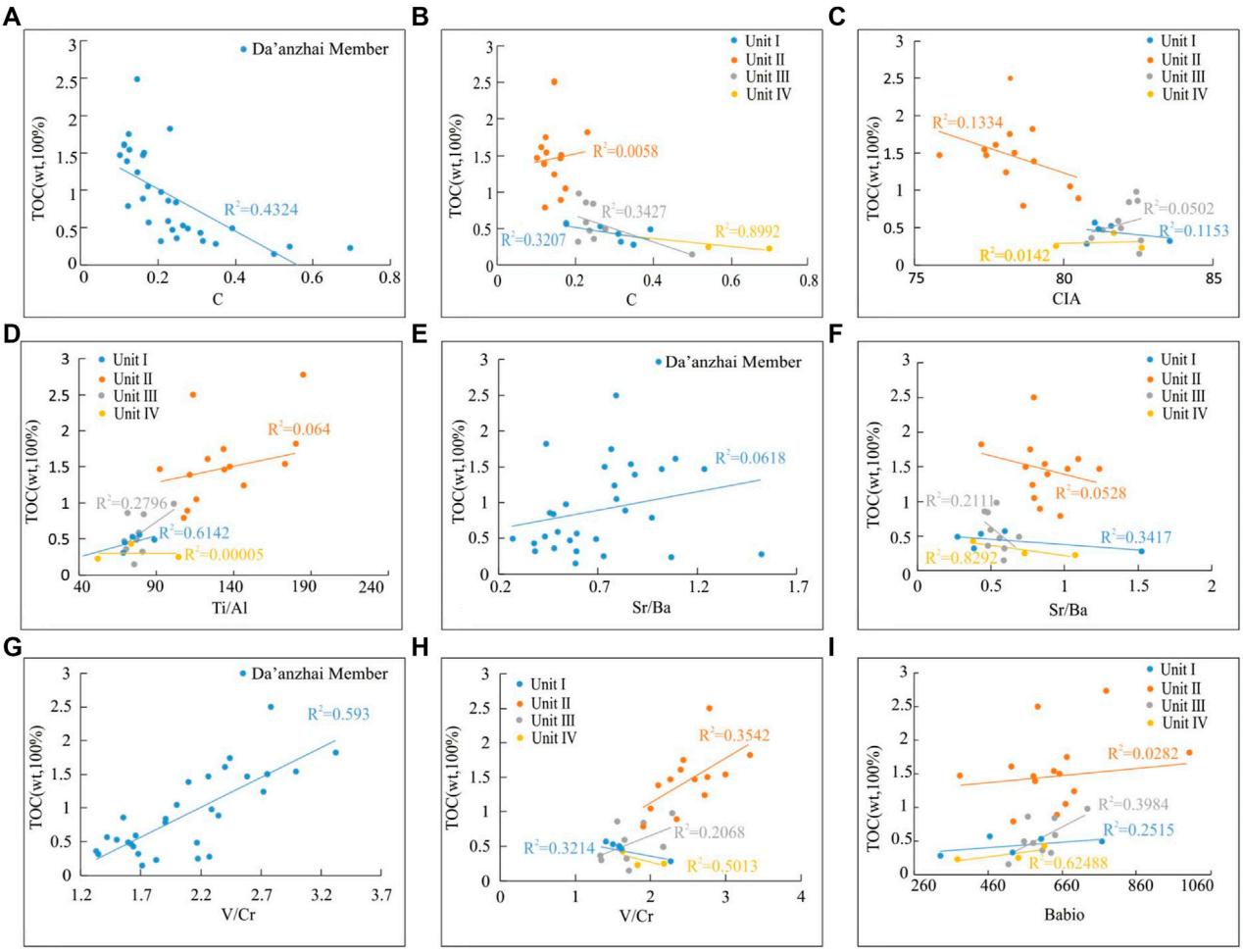

FIGURE 8
Cross-plot of environment parameter and TOC in the Da'anzhai member of well C. **(A)** Correlation between TOC and C in Da'anzhai Member; **(B)** Correlation between TOC and C in four small layers; **(C)** Correlation between TOC and CIA in four small layers; **(D)** Correlation between Ti/Al and C in four small layers; **(E)** Correlation between TOC and Sr/Ba in Da'anzhai Member; **(F)** Correlation between TOC and Sr/Ba in four small layers; **(G)** Correlation between TOC and V/Cr in Da'anzhai Member; **(H)** Correlation between TOC and Cr in four small layers; **(I)** Correlation between TOC and Babio in four small layers.

environment, while that of unit I is generally between 74.82 and 83.54, with an average of 79.85, indicating that the weathering degree is strengthened with the transition from unit II to unit I and the gradual wetting of climate.

From the correlation between the CIA and TOC (Figure 8C), the poor correlation between weathering and organic matter enrichment in various periods in the Da'anzhai member suggests that weathering has not significantly influenced organic matter enrichment.

5.3 Terrestrial input and hydrodynamic conditions

Considering that Si may be biogenic or terrestrial input, Si should be used carefully to evaluate paleoredox conditions (Zhao et al., 2016). Al mainly comes from aluminosilicate clay minerals (Arthur and Sageman, 1994), while Ti generally exists in clay and heavy minerals (Kidder and Erwin, 2001). The Ti/Al ratio provides an index to measure the transport energy of sediments (Murphy et al., 2000).

The Al, Ti, and Ti/Al curves reflect the variable terrestrial input in the Da'anzhai member (Figure 7). Continued high values in unit IV-III and unit I in the humid climatic zone indicate a high terrestrial input of the period. However, a short-term shift to low values in unit II in the arid climatic zone, and weathering is also weaker in unit II, which indicates a lower terrestrial input for the period (Figure 7), suggesting that terrestrial input is influenced by both paleoclimate and weathering. Deep lakes have lower input of terrigenous detrital, the climate became drier in unit I, and diagenetic minerals such as calcite and

dolomite dominated the deposition of the shale strata (Figure 3). The change of Ti/Al is contrary to that of Ti and Al from the lower part to the upper part of the Da'anzhai member. It is speculated that the changing trend of Al, Ti, and Ti/Al is opposite due to the enhancement of hydrodynamic force and energy input into the lake as the lake level retreats from the end of unit III to unit I.

In terms of the correlation between Ti/Al and TOC (Figure 8D), the poor or even negative correlation from all units' correlations indicates that terrestrial inputs have had a damaging effect on the preservation of organic matter. The weak correlation between Ti/Al and TOC in unit III can be speculated that the humid and warm climate accelerated the circulation of water vapor in the atmosphere, enhanced chemical weathering and surface runoff, and transported higher plants and organic matter into the lake (Figure 2G, Figure 2H). Terrigenous input indicators, such as the Ti/Al ratio, are used to indicate deposition rates. Generally, the higher the terrigenous input, the higher will be the deposition rate. The results show that the terrigenous input is the highest in the high TOC section (II), that is, the deposition rate is high. This may be due to a moist and warm climate that accelerates the circulation of water vapor in the atmosphere and enhances terrigenous weathering. In addition, terrigenous weathering, on the one hand, transported higher plants and organic matter to the lake (Figure 2G, Figure 2H), and on the other hand, imported a large number of nutrient elements, which promoted the productivity of the lake.

5.4 Paleosalinity

Paleosalinity refers to the salinity preserved in paleosediments, which is an important symbol indicating the change in the sedimentary environment in geological history. Because the migration ability of Sr and the solubility of its sulfate compounds are far greater than that of Ba, strontium and barium appear in the form of soluble bicarbonates in natural water when the salinity is low. When the water salinity gradually increases, Ba first precipitates into $BaSO_4$, resulting in the enrichment of Sr relative to Ba. Sr precipitates to $SrSO_4$ only when the water body is further salted, so Sr/Ba is usually used to divide the salinity of the water body (Zheng and Liu, 1999). The study of continental lake basins showed that for Sr/Ba ratios greater than 1.0, the lake is salt water, for ratios between 1.0 and 0.5, the lake is semi-saltwater, and for ratios less than 0.5, the lake is fresh water.

According to the changing trend of Sr/Ba in unit IV-II (Figure 7), the water gradually becomes salinized from freshwater from unit IV-III. In unit II, it is from semi-saltwater to salt water. In unit I, although the lake level drops further, the climate becomes warm and humid, and the Sr/Ba value is generally lower than 1, which has the characteristics of freshwater.

From the correlation between the TOC and Sr/Ba (Figure 8E), salinity correlates poorly with TOC, indicating that lake salinity has little correlation with organic matter enrichment and too low salinity is not suitable for organic matter enrichment. According to the correlation between TOC and Sr/Ba in different periods (Figure 8F), the unit II has the characteristics of high salinity and high TOC compared with the unit IV-III and the unit I, which indicates that appropriate salinity is beneficial to the enrichment of organic matter under the background of high drought. However, the correlation between TOC and Sr/Ba in unit II is poor, which indicates that salinity is not the most important factor affecting organic matter enrichment in unit II.

5.5 Redox condition

Redox-sensitive trace elements (RSTEs, such as Mo, U, and V) have dissolution or sedimentation characteristics under different redox conditions, so that the redox condition of the paleoenvironment can be restored by RSTEs (Tribovillard et al., 2006). Whether the RSTEs are terrestrial input or not needs to be evaluated first. The correlation coefficient between Mo_{EF}, U_{Ef}, and A1 is 0.69 and 0.72. However, the correlation coefficient between V_{EF} and Al concentration is only 0.0064. It is proved that the V is not from terrestrial input. So, it is reliable to use V to characterize the redox condition. V_{EF} lower than 1 means the depletion of V, showing the developmental oxidation environment of the Da'anzhai member (Figure 7).

The redox sensitivity rate (TEs), such as the trace element ratio such as U/Th, V/Cr, and Ni/Co, is also used to show the oxidation–reduction properties of water. The lower the ratio, the higher the oxidation degree of water is; the higher the ratio, the higher the reduction degree of water is (Hatch and Leventhal, 1992; Jones and Manning, 1994; Tribovillard et al., 2006). According to the trace element ratio, the oxidation–reduction properties of water can be divided into three levels: oxidized state, sub-oxidized state, and reduction state (Figure 9) (Jones and Manning, 1994). The ratio casting point of various elements (Figure 9) shows that most of the data points of Ni/Co are in the oxidized and sub-oxidized zone. V/Cr can identify the redox environment of mudstone effectively. V/Cr<2.00 represents the oxidizing environment; 2.00<V/Cr<4.25 represents the semi-reductive environment; and V/Cr>4.25 represents the anoxic environment. V/Cr indicates unit IV-III and unit I are in an oxidizing environment (Figure 7), and the V/Cr of unit II is 2–4.25, which shows unit II is in a semi-reductive state. It is consistent with the development of pyrite in unit II (Figure 3).

There is a favorable correlation between the TOC and V/Cr according to the intersection diagram (Figure 8G). It shows that the redox condition is the main factor in controlling organic matter enrichment in the Da'anzhai member. However, in unit

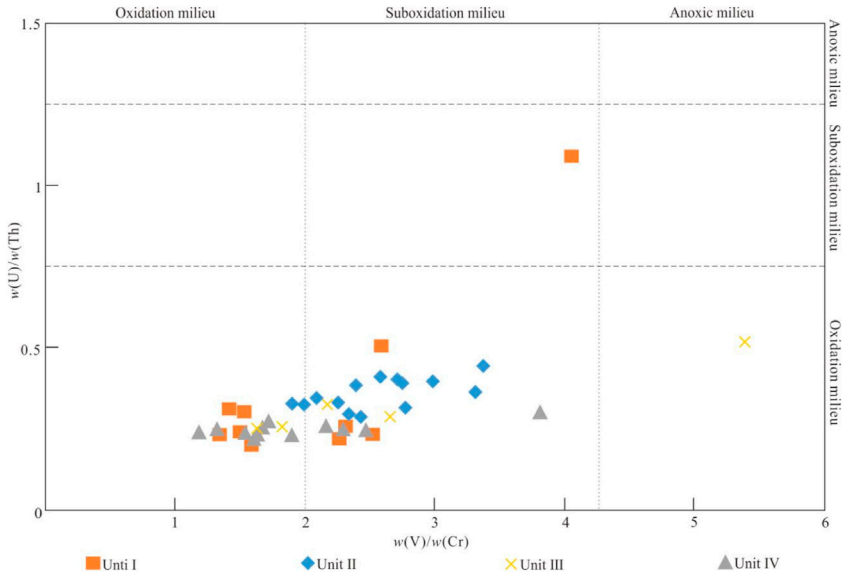

FIGURE 9
Intersection diagram of trace element ratio in the Da'anzhai member.

III, there is a weak correlation between the TOC and V/Cr (Figure 8H). In previous studies, the sediment of high TOC can be formed if there is enough organic matter in the non-reductive environment (Pedersen and Calvert, 1990). Abundant organic matter can consume a lot of oxygen when decomposing. It can cause anoxia in the water ground, which is in favor of storing the organic matter (Pedersen and Calvert, 1990; Wei et al., 2012). There is a negative correlation between unit IV, unit I, and TOC (Figure 8H), which shows that the organic matter enrichment of the two members does not control by the oxidation–reduction environment.

5.6 Paleoproductivity

Excess of Ba_{bio}, Cu, Ni, and P in shale has been used in studying the strength of paleoproductivity. Under the reduction condition, Ni and Cu are the ideal indexes for entering the sediments (Tribovillard et al., 2006). There exist many disputes in the P element indicating the change of paleoproductivity, which concentrates on the different correlations between biological P (organophosphorus) and productivity (Slomp et al., 2002; Ma et al., 2008). In the anoxic environment, the sulfate reduction reaction is generally released on the sediment surface and water ground. Barium sulfate is one type of sulfate, and partial dissolution of barium sulfate will make the content value of the tested barium smaller, which causes the estimated productivity to become lower (Calvert and Pedersen, 2007). The previous study has proved that water, which is in the sediment period of the black rock series in the Da'anzhai member of the studied area, is in an oxidizing and semi-oxidizing (semi-reductive) environment. There were no hydrothermal activities in the Jurassic sedimentary period in the Sichuan Basin. In the meanwhile, the concurrent variation trend of the content of Ba and Ba_{bio} in the vertical direction shows that Ba in the studied area is mainly from a biological source (Figure 8). The biological source of barium can be the paleoproductivity index. So, the study takes Ba_{bio} to characterize the production capacity.

Ba_{bio} in the Da'anzhai member of the studied area changed relatively significantly and its distributing range is 330.80–3556.12 ppm, with an average of 647.963 ppm. According to the productivity index (Figure 7), with the lake level rising, terrestrial input of unit IV-III in that period was relatively large and more nutrients had been taken into the lake; unit II was under the arid and anoxic environment and it is in favor of the enrichment of nutrients such as P in the water of lakes (Van Cappellen and Ingall, 1994). Moreover, the decomposition of a large number of bivalve shells after extinction can promote the eutrophication of water (Zhang et al., 2016). In general, in the mildly saline water with Sr/Ba in 0.5–0.8, algae bloomed (Jiao, 2019), and the productivity was relatively high, which made the lakes have productivity to a certain extent. It was consistent with most saltwater lakes in the world which have high productivity. It is reported that the salt content of the northern Great Salt Lake in Utah State is 22%. There are large quantities of algae and heterotrophic bacterium in the lake. Therefore, the Great Salt Lake in Utah State has great productivity. The productivity of unit I is the lowest. It is related to the large decline of the lake level, which leads to the overall oxidation environment of the lake and the difficulty of preserving organic matter.

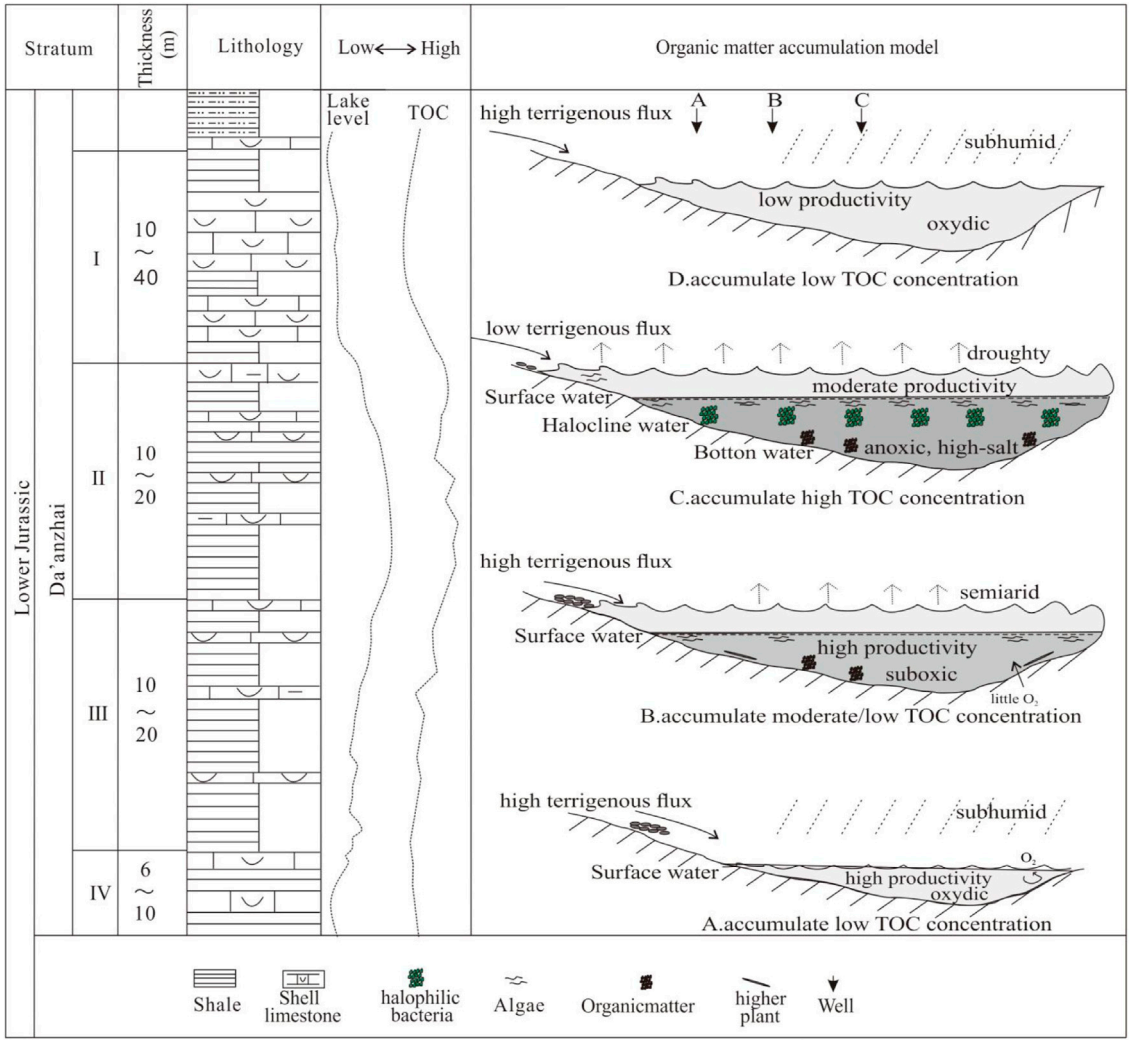

FIGURE 10
Organic matter enrichment pattern of the Da'anzhai member in Sichuan Basin.

According to the correlation between the TOC and Ba_{bio} (Figure 8I), they have different correlations in different periods. In unit IV and unit III, the correlation coefficient between TOC and Ba_{bio} are 0.62 and 0.39, respectively, which shows that the two indicators have a favorable correlation; in unit I, the correlation coefficient between TOC and Ba_{bio} is just 0.25 and it has a relatively weak correlation; the correlation coefficient between unit II and TOC is just 0.02 and it has a poor correlation.

5.7 Organic matter enrichment pattern

According to the various sedimentary environment parameters discussed in the previous study, the author induced the organic matter enrichment pattern of the Da'anzhai member in the Sichuan Basin (Figure 10).

In unit IV-III, during this period, the lake level gradually increased; at the end of unit III, it increased to the largest lake flooding surface; the water in unit IV is relatively shallow, and the lakes are relatively open, which forms the oxidation environment; with rising of the lake level, the lakes gradually become sealing, which forms the semi-oxidized environment. Even the oxidation environment is unfavorable to the preservation and enrichment of organic matter, units IV-III have developed a semi-humid and semi-arid climatic environment and freshwater has been inlet by precipitation and surface runoff. It not only brings organic matter such as plant debris but also provides consumption to the primary producer such as surficial algae by inletting large amounts of dissolved substances as nutriment. The type III organic matter preservation pattern has formed in this period, which is controlled by productivity.

In unit II, the climate gradually becomes arid, and the lake level gradually declines after it achieves the largest lake flooding surface; freshwater supply in the basin decreases rapidly, which leads to the fresh lakes gradually becoming salified. Due to the density difference, lake water forms a stable salt layering environment. Water salinity in the shallow stratum is low and the oxidation rate is high. A large number of algae and phytoplankton have developed, which improves the primary producer of the unit. Water salinity in the mid-deep stratum may change with the change in the paleoclimate and halophilic bacteria may propagate a lot in this unit; under the condition, the dissolved oxygen has been consumed rapidly and the anoxic environment has been formed. Due to the arid climate and the poor inlet of freshwater, lake stratification was stagnant, which led the middle and lower parts to the anoxic saline state in a long term. Because of the anoxic state, phosphorus and other nutrients have been recycled into the water effectively (Van Cappellen and Ingall, 1994), and the water becomes eutrophicated. In addition, the mineral content of clay in the unit is relatively high (Figure 3), which can absorb the organic matter effectively (Xu et al., 2017). In general, the relatively high primary productivity and preserving condition in that period formed the type II organic matter enrichment pattern which biases toward a reduction condition. What is worth paying attention to is that the accumulation of organic matter in the lake basin in the Da'anzhai member of the Sichuan Basin is relatively lower than that in other lake basins in the world. It may refer to the gravity flow development of the unit, which is unfavorable to organic matter preservation to a certain extent. It leads the TOC in unit II to be relatively lower than the organic matter sedimentation of other lakes in the world.

In general, unit I is the period in which the range of the lake is the minimum in the Da'anzhai member. In that stage, the hydrodynamic is strong and the amount of dissolved oxygen in water has increased, which appears in an oxidation environment; in the meanwhile, with the decline in the lake level, the increasing terrestrial input restricts organic matter enrichment, and organic matter accumulation is relatively less.

6 Conclusion

Through comprehensive studies of the sedimentology and geochemistry of the Da'anzhai member in the late Early Jurassic in the Sichuan Basin, the author has a new understanding of the organic matter disposition mechanisms of the unit. In the Da'anzhai member, the organic matter in unit II is the most enriched and that in unit III is sub-enrichment. The formation of the two organic-rich shales is not referring to a single factor. It refers to the mutual coupling of paleoclimate, redox properties, productivity, paleosalinity, and many other factors.

Under a semi-humid and semi-arid environment, the chemical degree of weathering is relatively high in unit III of the Da'anzhai member, and it inlets many nutrients into lakes, such as higher plants. The productivity is relatively high in that period and formed the organic matter enrichment pattern which biases toward the oxidized condition.

Under the arid environment, freshwater supply decreases rapidly in unit II of the Da'anzhai member, which leads the fresh lake gradually to become salified. Because of the density difference, lake water forms a stable salt layering environment, and it is oxygen enriched on the surface, with low salinity and extensively develops phytoplankton and algae. Its primary productivity is high; in the middle and lower parts, it is anoxic and the salinity is high; phosphorus and other nutrients have been effectively recycled into the water which caused the water to be eutrophicated. Unit II is in a semi-reduction environment and it is the ideal place for organic matter enrichment. Therefore, it formed the organic matter enrichment pattern biases toward the reductive condition.

Data availability statement

The raw data supporting the conclusion of this article will be made available by the authors, without undue reservation.

Author contributions

YD and XW designed experiments; CC, SW, RT, QM, and JZ carried out experiments; RZ, YZ, and SHanalyzed experimental results. YD wrote the manuscript.

Acknowledgments

We thank Qian Pang of State Key Laboratory of Oil and Gas Reservoir Geology and Exploitation, Southwest Petroleum University for his support in field section positioning and field discussion. The authors appreciate the reviewers who gave constructive suggestions which polished the paper so much.

Conflict of interest

YD, CC, SW, RT, QM, JZ, and YZ were employed by the company Exploration Division of Petro China Southwest Oil and Gasfield Company. SH was employed by the company CNPC.

The remaining author declares that the research was conducted in the absence of any commercial or financial relationships that could be construed as a potential conflict of interest.

Publisher's note

References

Arthur, M. A., and Sageman, B. B. (1994). Marine black shales: Depositional mechanisms and environments of ancient deposits. *Annu. Rev. Earth Planet. Sci.* 22 (1), 499–551. doi:10.1146/annurev.ea.22.050194.002435

Bluth, G. J., and Kump, L. R. (1994). Lithologic and climatologic controls of river chemistry. *Geochimica Cosmochimica Acta* 58 (10), 2341–2359. doi:10.1016/0016-7037(94)90015-9

Calvert, S. E. (1987). Oceanographic controls on the accumulation of organic matter in marine sediments. *Mar. Pet. Source Rocks* 26 (1), 137–151. doi:10.1144/gsl.sp.1987.026.01.08

Calvert, S. E., and Pedersen, T. F. (2007). Chapter fourteen elemental proxies for palaeoclimatic and palaeoceanographic variability in marine sediments: Interpretation and application. *Dev. Mar. Geol.* 1, 567–644. doi:10.1016/s1572-5480(07)01019-6

Demaison, G. J., and Moore, G. T. (1980). Anoxic environments and oil source bed Genesis. *AAPG Bull.* 64 (8), 1179–1209.

Deng, S. H., Lu, Y. Z., Zhao, Y., Fan, R., Wang, Y., Yang, X., et al. (2017). The Jurassic palaeoclimate regionalization and evolution of China. *Earth Sci. Front.* 24 (1), 106–142. doi:10.13745/j.esf.2017.01.007

Dymond, J., Suess, E., and Lyle, M. (1992). Barium in deep-sea sediment: A geochemical proxy for paleoproductivity. *Paleoceanography* 7 (2), 163–181. doi:10.1029/92pa00181

Hatch, J. R., and Leventhal, J. S. (1992). Relationship between inferred redox potential of the depositional environment and geochemistry of the upper pennsylvanian (missourian) Stark shale member of the dennis limestone, wabaunsee county, Kansas, USA. *Chem. Geol.* 99 (1-3), 65–82. doi:10.1016/0009-2541(92)90031-y

Hu, D. F., Wei, Z. H., Liu, R. B., Wei, X., and Chen, F. (2021). Enrichment control factors and exploration potential of lacustrine shale oil and gas:A case study of Jurassic in the Fuling area of the Sichuan Basin. *Nat. Gas. Ind. B* 41 (8), 1–8. doi:10.1016/j.ngib.2021.08.012

Huang, Z., Wang, X., Yang, X., Zhu, R., Cui, J., Shi, W., et al. (2020). Paleoenvironment and organic matter accumulation of the upper ordovician-lower silurian, in upper yangtze region, South China: Constraints from multiple geochemical proxies. *Energies* 13 (4), 858–916. doi:10.3390/en13040858

Jiao, F. Z. (2019). Re-recognition of "unconventional" in unconventional oil and gas. *Petroleum Explor. Dev.* 46 (5), 847–855. doi:10.1016/s1876-3804(19)60244-2

Jinhua, F. U., Shixiang, L. I., Liming, X. U., and Niu, X. (2018). Paleo-sedimentary environmental restoration and its significance of chang 7 member of triassic yanchang formation in ordos basin, NW China. *Petroleum Explor. Dev.* 45 (6), 998–1008. doi:10.1016/s1876-3804(18)30104-6

Jones, B., and Manning, D. A. (1994). Comparison of geochemical indices used for the interpretation of palaeoredox conditions in ancient mudstones. *Chem. Geol.* 111 (1-4), 111–129. doi:10.1016/0009-2541(94)90085-x

Kidder, D. L., and Erwin, D. H. (2001). Secular distribution of biogenic silica through the phanerozoic: Comparison of silica-replaced fossils and bedded cherts at the series level. *J. Geol.* 109 (4), 509–522. doi:10.1086/320794

Li, X., Wang, J., Rasbury, T., Zhou, M., Wei, Z., and Zhang, C. (2020). Early Jurassic climate and atmospheric CO_2 concentration in the Sichuan paleobasin, southwestern China. *Clim. Past.* 16 (6), 2055–2074. doi:10.5194/cp-16-2055-2020

Li, Y., and He, D. (2014). Evolution of tectonic-depositional environment and prototype basins of the Early Jurassic in Sichuan Basin and adjacent areas. *Acta Pet. Sin.* 35 (2), 219–232. doi:10.7623/syxb201402002

Liu, J., Cao, J., Hu, G., Wang, Y., Yang, R., and Liao, Z. (2020). Water-level and redox fluctuations in a Sichuan Basin lacustrine system coincident with the Toarcian OAE. *Palaeogeogr. Palaeoclimatol. Palaeoecol.* 558, 109942. doi:10.1016/j.palaeo.2020.109942

Liu, S. G. (1993). *The formation and evolution of Longmenshan thrust zone and western Sichuan*. China. Chengdu: Press of Chengdu University of Science and Technology.

Loucks, R. G., and Ruppel, S. C. (2007). Mississippian barnett shale: Lithofacies and depositional setting of a deep-water shale-gas succession in the fort worth basin, Texas. *Am. Assoc. Pet. Geol. Bull.* 91 (4), 579–601. doi:10.1306/11020606059

Ma, Z. W., Chaoyong, H., Jiaxin, Y., and Xinong, X. (2008). Biogeochemical records at Shangsi section, northeast Sichuan in China: The Permian paleoproductivity proxies. *J. China Univ. Geosciences* 19 (5), 461–470. doi:10.1016/s1002-0705(08)60051-5

Mayer, L. M., Rahaim, P. T., Guerin, W., Macko, S. A., Watling, L., and Anderson, F. E. (1985). Biological and granulometric controls on sedimentary organic matter of an intertidal mudflat. *Estuar. Coast. Shelf Sci.* 20 (4), 491–503. doi:10.1016/0272-7714(85)90091-5

McLennan, S. M., Hemming, S., McDaniel, D. K., and Hanson, G. N., (1993). Geochemical approaches to sedimentation, provenance, and tectonics. *Special Papers-Geological Soc. Am.* 284, 21–40. doi:10.1130/SPE284-p21

Meng, F., Chen, H., and Li, X. (2005). Study on lower-middle jurassic boundary in chongqing region. *Geol. Mineral Resour. South China* 3, 64–71. doi:10.3969/j.issn.1007-3701.2005.03.013

Moradi, A. V., Sarı, A., and Akkaya, P. (2016). Geochemistry of the Miocene oil shale (Hançili Formation) in the Çankırı-Çorum Basin, Central Turkey: Implications for Paleoclimate conditions, source–area weathering, provenance and tectonic setting. *Sediment. Geol.* 341, 289–303. doi:10.1016/j.sedgeo.2016.05.002

Murphy, A. E., Sageman, B. B., Hollander, D. J., Lyons, T. W., and Brett, C. E. (2000). Black shale deposition and faunal overturn in the Devonian Appalachian Basin: Clastic starvation, seasonal water-column mixing, and efficient biolimiting nutrient recycling. *Paleoceanography* 15 (3), 280–291. doi:10.1029/1999pa000445

Nesbitt, H., and Young, G. M. (1982). Early Proterozoic climates and plate motions inferred from major element chemistry of lutites. *Nature* 299 (5885), 715–717. doi:10.1038/299715a0

Pedersen, T. F., and Calvert, S. E. (1990). Anoxia vs. productivity: What controls the formation of organic-carbon-rich sediments and sedimentary rocks? *AAPG Bull.* 74 (4), 454–466.

Slomp, C. P., Thomson, J., and Lange, G. J. (2002). Enhanced regeneration of phosphorus during formation of the most recent eastern Mediterranean sapropel (S1). *Geochimica Cosmochimica Acta* 66 (7), 1171–1184. doi:10.1016/s0016-7037(01)00848-1

Taylor, S. R., and Mclennan, S. M. (1985). *T*he continental crust: Its composition andevolution. London: Blackwell Scientific Publications.

Tong, Z., Shengxiang, L., and Feng, W. (2016). Sedimentary models and lithofacies types of lacustrine mud shale in the Sichuan Basin. *Nat. Gas. Ind.* 36 (8), 22–28. doi:10.3787/j.issn.1000-0976.2016.08.003

Tribovillard, N., Algeo, T. J., Baudin, F., and Riboulleau, A. (2012). Analysis of marine environmental conditions based onmolybdenum–uranium covariation—applications to mesozoic paleoceanography. *Chem. Geol.* 324-325, 46–58. doi:10.1016/j.chemgeo.2011.09.009

Tribovillard, N., Algeo, T. J., Lyons, T., and Riboulleau, A. (2006). Trace metals as paleoredox and paleoproductivity proxies: An update. *Chem. Geol.* 232 (1-2), 12–32. doi:10.1016/j.chemgeo.2006.02.012

Turekian, K. K., and Wedepohl, K. H. (1961). Distribution of the elements in some major units of the earth's crust. *Geol. Soc. Am. Bull.* 72 (2), 175–192. doi:10.1130/0016-7606(1961)72[175:doteis]2.0.co;2

Van Cappellen, P., and Ingall, E. D. (1994). Benthic phosphorus regeneration, net primary production, and ocean anoxia: A model of the coupled marine biogeochemical cycles of carbon and phosphorus. *Paleoceanography* 9 (5), 677–692. doi:10.1029/94pa01455

Wang, Y., Xu, S., Hao, F., Poulton, S. W., Zhang, Y., Guo, T., et al. (2021). Arid climate disturbance and the development of salinized lacustrine oil shale in the Middle Jurassic Dameigou Formation, Qaidam Basin, northwestern China. *Palaeogeogr. Palaeoclimatol. Palaeoecol.* 577, 110533. doi:10.1016/j.palaeo.2021.110533

Wedepohl, K. H. (1971). Environmental influences on the chemical composition of shales and clays. *Phys. Chem. Earth* 8, 307–333. doi:10.1016/0079-1946(71)90020-6

Wei, H., Chen, D., Wang, J., Yu, H., and Tucker, M. E. (2012). Organic accumulation in the lower chihsia formation (middle permian) of South China: Constraints from pyrite morphology and multiple geochemical proxies. *Palaeogeogr. Palaeoclimatol. Palaeoecol.* 353, 73–86. doi:10.1016/j.palaeo.2012.07.005

Wu, Z., Zhao, X., Wang, E., Pu, X., Lash, G., Han, W., et al. (2021). Sedimentary environment and organic enrichment mechanisms of lacustrine shale: A case study of the paleogene shahejie formation, qikou sag, bohai bay basin. *Palaeogeogr. Palaeoclimatol. Palaeoecol.* 573, 110404. doi:10.1016/j.palaeo.2021.110404

Xu, J., Jin, Q., Xu, X., Cheng, F. Q., Hu, C. H., Wang, B., et al. (2021). Factors controlling organic-rich shale development in the liushagang formation, weixinan sag, beibu gulf basin: Implications of structural activity and the depositional environment. *Petroleum Sci.* 18 (4), 1011–1020. doi:10.1016/j.petsci.2020.08.001

Xu, Q., Liu, B., Ma, Y., Song, X., Wang, Y., and Chen, Z. (2017). Geological and geochemical characterization of lacustrine shale: A case study of the jurassic Da'anzhai member shale in the central sichuan Basin, southwest China. *J. Nat. Gas Sci. Eng.* 47, 124–139. doi:10.1016/j.jngse.2017.09.008

Zhang, F., Zhou, Y. X., and Ge, R. Q., (2018). A new type of lacustrine ichnofossils from the Lower Jurassic Ziliujing Formation in Wanzhou of Chongqing and its paleoenvironmental significances. *Acta Palaeontol. Sin.* 57 (2), 228–236. doi:10.19800/j.cnki.aps.2018.02.008

Zhang, H., Wu, X., and Wang, B., (2016). Research progress of the enrichment mechanism of sedimentary organics in lacustrine basin. *Acta Sedimentol. Sin.* 34 (3), 463–477. doi:10.14027/j.cnki.cjxb.2016.03.004

Zhang, J. C., Lin, L. M., and Li, Y. X., (2012). Classification and evaluion of shale oil. *Earth Front.* 19 (5), 322–331.

Zhao, J., Jin, Z., Jin, Z., Geng, Y., Wen, X., and Yan, C. (2016). Applying sedimentary geochemical proxies for paleoenvironment interpretation of organic-rich shale deposition in the Sichuan Basin, China. *Int. J. Coal Geol.* 163, 52–71. doi:10.1016/j.coal.2016.06.015

Zhao, W. Z., Zhu, R. K. Z., Hu, S. Y., Hou, L., and Wu, S. (2020). Accumulation contribution differences between lacustrine organic-rich shales and mudstones and their significance in shale oil evaluation. *Petroleum Explor. Dev.* 47 (6), 1160–1171. doi:10.1016/s1876-3804(20)60126-x

Zheng, R. (1998). High-resolution sequence stratigraphy of Da'anzhai formation, lower jurassic in sichuan Basin. *Acta Sedimentol. Sin.* 16, 42–49.

Zheng, R. C., and Liu, M. Q. (1999). Study on palaeosalinity of Chang-6 oil reservoir set in Ordos Basin. *Oil Gas Geol.* 20 (1), 20–25.

Zou, C. N., Yang, Z., Wang, H. Y., et al. (2019). Exploring petroleum inside source kitchen": Jurassic unconventional continental giant shale oil & gas field in Sichuan basin, China. *Acta Geol. Sin.* 93 (7), 1551–1562. doi:10.19762/j.cnki.dizhixuebao.2019188